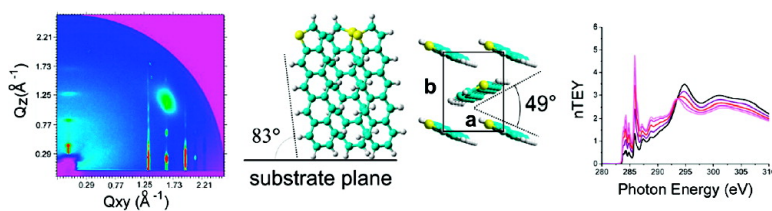


## Thin Film Structure of Tetraceno[2,3-*b*]thiophene Characterized by Grazing Incidence X-ray Scattering and Near-Edge X-ray Absorption Fine Structure Analysis

Quan Yuan, Stefan C. B. Mannsfeld, Ming L. Tang, Michael F. Toney, Jan Lning, and Zhenan Bao

*J. Am. Chem. Soc.*, 2008, 130 (11), 3502-3508 • DOI: 10.1021/ja0773002

Downloaded from <http://pubs.acs.org> on February 8, 2009



### More About This Article

Additional resources and features associated with this article are available within the HTML version:

- Supporting Information
- Links to the 5 articles that cite this article, as of the time of this article download
- Access to high resolution figures
- Links to articles and content related to this article
- Copyright permission to reproduce figures and/or text from this article

[View the Full Text HTML](#)

## Thin Film Structure of Tetraceno[2,3-*b*]thiophene Characterized by Grazing Incidence X-ray Scattering and Near-Edge X-ray Absorption Fine Structure Analysis

Quan Yuan,<sup>†</sup> Stefan C. B. Mannsfeld,<sup>\*‡</sup> Ming L. Tang,<sup>§</sup> Michael F. Toney,<sup>||</sup>  
Jan Lüning,<sup>||</sup> and Zhenan Bao<sup>\*‡</sup>

Department of Materials Science and Engineering, Department of Chemical Engineering, and Department of Chemistry, Stanford University, California 94305, and Stanford Synchrotron Radiation Laboratory, Stanford Linear Accelerator Center, 2575 Sand Hill Road, M/S 69, Menlo Park, California 94025

Received September 27, 2007; E-mail: mannsfel@stanford.edu; zbao@stanford.edu

**Abstract:** Understanding the structure–property relationship for organic semiconductors is crucial in rational molecular design and organic thin film process control. Charge carrier transport in organic field-effect transistors predominantly occurs in a few semiconductor layers close to the interface in contact with the dielectric layer, and the transport properties depend sensitively on the precise molecular packing. Therefore, a better understanding of the impact of molecular packing and thin film morphology in the first few monolayers above the dielectric layer on charge transport is needed to improve the transistor performance. In this Article, we show that the detailed molecular packing in thin organic semiconductor films can be solved through a combination of grazing incidence X-ray diffraction (GIXD), near-edge X-ray absorption spectra fine structure (NEXAFS) spectroscopy, energy minimization packing calculations, and structure refinement of the diffraction data. We solve the thin film structure for 2 and 20 nm thick films of tetraceno[2,3-*b*]thiophene and detect only a single phase for these thicknesses. The GIXD yields accurate unit cell dimensions, while the precise molecular arrangement in the unit cell was found from the energy minimization and structure refinement; the NEXAFS yields a consistent molecular tilt. For the 20 nm film, the unit cell is triclinic with  $a = 5.96 \text{ \AA}$ ,  $b = 7.71 \text{ \AA}$ ,  $c = 15.16 \text{ \AA}$ ,  $\alpha = 97.30^\circ$ ,  $\beta = 95.63^\circ$ ,  $\gamma = 90^\circ$ ; there are two molecules per unit cell with herringbone packing (49–59° angle) and tilted about 7° from the substrate normal. The thin film structure is significantly different from the bulk single-crystal structure, indicating the importance of characterizing thin film to correlate with thin film device performance. The results are compared to the corresponding data for the chemically similar and widely used pentacene. Possible effects of the observed thin film structure and morphology on charge carrier mobility are discussed.

### Introduction

Oligomeric organic semiconductor molecules are attracting research interest due to their potential applications for low-cost electronics.<sup>1–6</sup> Much effort is directed toward gaining a better understanding of various factors influencing carrier mobility in

organic thin film transistors, which can be potentially manufactured by high throughput roll-to-roll processes. The highest p-type carrier mobility for thin film transistors has been reported for vacuum-deposited pentacene thin film transistors (greater than  $5 \text{ cm}^2 \text{ V}^{-1} \text{ s}^{-1}$ ).<sup>7</sup> Many heteroacenes and pentacene derivatives have been synthesized to further improve the charge carrier mobility, chemical stability, and solubility.<sup>8–14</sup> Although electronic properties are easily tuned by molecular design, the relationship between molecular structure and thin film morphol-

<sup>†</sup> Department of Materials Science and Engineering, Stanford University.

<sup>‡</sup> Department of Chemical Engineering, Stanford University.

<sup>§</sup> Department of Chemistry, Stanford University.

<sup>||</sup> Stanford Linear Accelerator Center.

- (1) Bao, Z.; Locklin, J. J. *Organic field-effect transistors*; CRC Press: Boca Raton, FL, 2007.
- (2) Klauk, H.; Zschieschang, U.; Pflaum, J.; Halik, M. *Nature* **2007**, *445*, 745–748.
- (3) Sheraw, C. D.; Zhou, L.; Huang, J. R.; Gundlach, D. J.; Kane, M. G.; Hill, I. G.; Hammond, M. S.; Campi, J.; Greening, B. K.; Francl, J.; West, J.; Jackson, T. N. *Appl. Phys. Lett.* **2002**, *80*, 1088–1090.
- (4) Rogers, J. A.; Bao, Z.; Baldwin, K.; Dodabalapur, A.; Crone, B.; Raju, V. R.; Kuck, V.; Katz, H.; Amundson, K.; Ewing, J.; Drzaic, P. *Proc. Natl. Acad. Sci. U.S.A.* **2001**, *98*, 4835–4840.
- (5) Siringhaus, H.; Kawase, T.; Friend, R. H.; Shimoda, T.; Inbasekaran, M.; Wu, W.; Woo, E. P. *Science* **2000**, *290*, 2123–2126.
- (6) Gelinck, G. H.; Huitema, H. E. A.; Veenendaal, E.; Cantatore, E.; Schrijnemakers, L.; Putten, J. B. P. H. v.; Geuns, T. C. T.; Beenhakkers, M.; Giesbers, J. B.; Huisman, B.; Meijer, E. J.; Benito, E. M.; Touwslager, F. J.; Marsman, A. W.; Rens, B. J. E. v.; Leeuw, D. M. d. *Nat. Mater.* **2004**, *3*, 106–110.

- (7) Kelley, T. W.; Muires, D. V.; Baude, P. F.; Smith, T. P.; Jones, T. D. *Mater. Res. Soc. Symp. Proc.* **2003**, *771*, L.6.5.1.
- (8) Anthony, J. E. *Chem. Rev.* **2006**, *106*, 5028–5048.
- (9) Tang, M. L.; Okamoto, T.; Bao, Z. *J. Am. Chem. Soc.* **2006**, *128*, 16002–16003.
- (10) Okamoto, T.; Senatore, M.; Ling, M. M.; Tang, M. L.; Bao, Z. *Adv. Mater.* **2007**, *19*, 3381–3384.
- (11) Anthony, J. E.; Brooks, J. S.; Eaton, D. L.; Parkin, S. R. *J. Am. Chem. Soc.* **2001**, *123*, 9482–9483.
- (12) Meng, H.; Sun, F.; Goldfinger, M. B.; Jaycox, G. D.; Li, Z.; Marshall, W. J.; Blackman, G. S. *J. Am. Chem. Soc.* **2005**, *127*, 2406–2407.
- (13) Meng, H.; Sun, F.; Goldfinger, M. B.; Gao, F.; Londono, D. J.; Marshall, W. J.; Blackman, G. S.; Dobbs, K. D.; Keys, D. E. *J. Am. Chem. Soc.* **2006**, *128*, 9304–9305.
- (14) Laquindanum, J. G.; Katz, H. E.; Lovinger, A. J. *J. Am. Chem. Soc.* **1998**, *120*, 664–672.

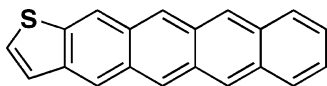


**Figure 1.** Chemical structure of tetraceno[2,3-*b*]thiophene (thiotetracene).

ogy and molecular packing structure is not yet well understood.<sup>15–17</sup> It is known that the molecular packing and film morphology in the first few monolayers near the semiconductor/dielectric interface, both of which are sensitive to processing conditions and molecular structure, strongly affect the transistor performance.<sup>18,19</sup> More experimental and theoretical work is needed to gain detailed understanding of the interplay between these factors.

Most previous structural characterizations were performed on bulk crystals, and these bulk structures were used to correlate with thin film charge transport properties.<sup>20</sup> However, thin film structures may be significantly different from bulk crystal structures. For example, in pentacene thin films the film structure is known to be significantly different from its bulk structure.<sup>19,21–23</sup> To directly correlate molecular structure with thin film charge transport properties, it is crucial to obtain the detailed structure of the organic semiconductor in thin film form. A number of groups have applied grazing incidence X-ray diffraction (GIXD) to elucidate the thin film unit cell structures of organic semiconductors,<sup>19,21,24</sup> while near-edge X-ray absorption fine structure (NEXAFS) spectroscopy has been used to provide information on average molecular tilt angle in thin films.<sup>25,26</sup> Detailed molecular arrangement has been calculated for pentacene by fitting grazing incidence crystal truncation rod (GICTR).<sup>27</sup> A combined effort using different characterization techniques to understand the molecular arrangement details in thin films will provide a more in-depth understanding for materials' microstructures.

In this work, we show that a combination of GIXD, NEXAFS, energy minimization packing calculations, and modeling of the diffraction data can be used to determine molecular packing details in thin films of a rigid organic semiconductor. We applied this approach to our recently reported tetraceno[2,3-*b*]thiophene semiconductor (see Figure 1 for chemical structure),<sup>9</sup> in which the terminal benzene ring in pentacene is replaced by a thiophene ring. For simplicity, this is hereafter referred to as thiotetracene. This thin film organic semiconductor is important for several

reasons. First, it has a high field-effect mobility of 0.45 cm<sup>2</sup>/V·s.<sup>9</sup> Second, its chemical structure closely resembles that of pentacene, and it is of great interest to compare its thin film structure with that of pentacene. Third, it is of interest to investigate the effect of dielectric surface on the thin film structure for this asymmetric molecule. The structural characterization results are correlated with the respective thin film transistor performance (carrier mobility) to investigate the structure–property relationships.

## Experimental Section

The synthesis of thiotetracene was reported previously.<sup>9</sup> It was purified four times by sublimation under high vacuum (10<sup>−6</sup> Torr). Pentacene was purchased from Aldrich Chemical Co. and was vacuum sublimed once.

Three different types of substrate surface treatment were carried out on silicon substrates with a native oxide layer. One type of surface (plain) was prepared by rinsing the substrate with acetone and isopropyl alcohol and a subsequent UV ozone treatment for about 20 min. Two other surface types were prepared by chemically modifying the surface with monolayers of hexamethyldisilazane (HMDS) and octadecyltriethoxysilane (OTS) using procedures as described in an earlier paper.<sup>28</sup>

Thiotetracene films (2 and 20 nm) and pentacene films (40 nm) were thermally deposited under high vacuum (10<sup>−6</sup> Torr base pressure) at a deposition rate of 0.2 Å/s, as monitored by a quartz crystal microbalance (QCM). The substrate temperature was maintained either at room temperature or at 60 °C during deposition.

GIXD measurements were carried out at the Stanford Synchrotron Radiation Laboratory (SSRL) on beam line 11-3 with a photon energy of 12.73 keV. The diffraction patterns were recorded using a 2D image detector (MAR345) with a pixel size of 150 μm (2300 × 2300 pixels). The detector was located at a distance of 400.5 mm from the sample center. The GIXD samples were about 10 mm × 15 mm. The incidence angle was chosen in the range of 0.09°–0.12° to optimize the signal-to-background ratio. The diffraction patterns were distortion-corrected ( $\theta$ -dependent image distortion introduced by planar detector surface) before performing quantitative analysis on the images. The overall resolution in the GIXD experiments, dominated by the sample size, was about 0.06 Å<sup>−1</sup>.

To obtain molecular tilting information, NEXAFS spectra were collected from 2 and 20 nm thick thiotetracene films. These experiments were performed on beam line 10-1 at SSRL. The carbon K-edge spectra were collected in total electron yield (TEY) mode over the photon energy range from 260 to 400 eV at five different beam incidence angles (20°, 40°, 55°, 70°, and 90°). The dichroic ratio was calculated following the procedures described in literature.<sup>25,29,30</sup>

The electrical characterization of thin film transistor devices in top-contact geometry was performed under ambient conditions using a Keithley 4200SCS semiconductor parameter analyzer. The samples used for electrical characterization were prepared during the same run of film deposition as those samples used for GIXD and NEXAFS experiments. The field-effect mobility was calculated from the transistor transfer curves in the saturation regime.

The packing energy of a three-dimensional spherical cluster (50 Å diameter, 200 molecules) was modeled using the nonbonded energy terms from the Optimized Potential for Liquid Simulations (OPLS) molecular force field (electrostatic interactions neglected).<sup>31</sup> The molecules were assumed to retain the optimal geometry of an isolated molecule (geometry-optimized using the Parametric Model number 3

- (15) Mayer, A.; Ruiz, R.; Zhou, H.; Headrick, R.; Kazimirov, A.; Malliaras, G. *Phys. Rev. B* **2006**, *73*, 205307-1–5.
- (16) Locklin, J.; Roberts, M.; Mannsfeld, S. C. B.; Bao, Z. *Polym. Rev.* **2006**, *46*, 79–101.
- (17) Sung, A.; Ling, M. M.; Tang, M. L.; Bao, Z.; Locklin, J. *Chem. Mater.* **2007**, *19*, 2342–2351.
- (18) Dimitrakopoulos, C. D.; Malenfant, P. R. L. *Adv. Mater.* **2002**, *14*, 99–117.
- (19) Yang, H. C.; Shin, T. J.; Ling, M. M.; Cho, K. L.; Ryu, C. Y.; Bao, Z. *J. Am. Chem. Soc.* **2005**, *127*, 11542–11543.
- (20) Valiyev, F.; Hu, W.-S.; Chen, H.-Y.; Kuo, M.-Y.; Chao, I.; Tao, Y.-T. *Chem. Mater.* **2007**, *19*, 3018–3026.
- (21) Fritz, S. E.; Martin, S. M.; Frisbie, C. D.; Ward, M. D.; Toney, M. F. *J. Am. Chem. Soc.* **2004**, *126*, 4084–4085.
- (22) Mattheus, C. C.; Dros, A. B.; Baas, J.; Meetsma, A.; Boer, J. L. d.; Palstra, T. T. M. *Acta Crystallogr.* **2001**, *C57*, 939–941.
- (23) Kakudate, T.; Yoshimoto, N.; Saito, Y. *Appl. Phys. Lett.* **2007**, *90*, 0819031–0819033.
- (24) Chabiny, M. L.; Toney, M. F.; Kline, R. J.; McCulloch, L.; Heeney, M. *J. Am. Chem. Soc.* **2007**, *129*, 3226–3237.
- (25) DeLongchamp, D. M.; Sambasivan, S.; Fischer, D. A.; Lin, E. K.; Chang, P.; Murphy, A. R.; Frechet, J. M. J.; Subramanian, V. *Adv. Mater.* **2005**, *17*, 2340–2344.
- (26) DeLongchamp, D. M.; Ling, M. M.; Jung, Y.; Fischer, D. A.; Roberts, M. E.; Lin, E. K.; Bao, Z. *J. Am. Chem. Soc.* **2006**, *128*, 16579–16586.
- (27) Schiefer, S.; Huth, M.; Dobrinevski, A.; Nickel, B. *J. Am. Chem. Soc.* **2007**, *129*, 10316–10317.

- (28) Locklin, J.; Ling, M. M.; Sung, A.; Roberts, M. E.; Bao, Z. *Adv. Mater.* **2006**, 2989–2992.
- (29) Stroh, J. *NEXAFS Spectroscopy*; Springer-Verlag: Berlin Heidelberg, 1992.
- (30) DeLongchamp, D. M.; Lin, E. K.; Fischer, D. A. *Proc. SPIE, San Diego* **2005**, 59400A-1–11.
- (31) Damm, W.; Frontera, A.; TiradoRives, J.; Jorgensen, W. *J. Comput. Chem.* **1997**, *18*, 1955–1970.

(PM3) semiempirical method). This rigid-molecule approximation drastically accelerates the convergence of the energy optimization and is a reasonable approximation for molecules with an extended delocalized  $\pi$ -electron system.<sup>31,32</sup> To simulate the influence of the inert substrate surface in this model, which was originally developed for bulk calculations, the two molecules in the unit cell were forced to sit in the empirically determined, thin film  $a$ – $b$  unit cell plane during the optimization.

## Results and Discussion

First, the experimental results obtained for 20 nm thick thiotetracene films are discussed and compared to theoretical calculations. Figure 2 shows the GIXD pattern of a 20 nm thick thiotetracene film grown at a substrate temperature of 60 °C on an OTS-treated Si substrate. As shown in Figure 2a, the diffraction data are presented as an intensity map in which the horizontal coordinate corresponds to the in-plane momentum transfer  $Q_{xy}$  and the vertical coordinate is the out-of-plane  $Q_z$  value. The diffraction image exhibits numerous out-of-plane diffraction peaks, which lie along constant  $Q_{xy}$ . This shows that the  $a$ – $b$  planes of thiotetracene crystallites are parallel to the interface with good registry between layers (along the  $\vec{c}$  direction).

The in-plane projection of Figure 2a is shown in Figure 2b. The (10L) and (01L) peaks are absent, while (12L) and (21L) exist, indicating a herringbone packing motif. The in-plane reciprocal lattice components were found to be independent of substrate temperature, surface treatment, and film thickness:  $a^*_{\parallel} = 1.06 \pm 0.03 \text{ \AA}^{-1}$ ,  $b^*_{\parallel} = 0.82 \pm 0.03 \text{ \AA}^{-1}$ ,  $\gamma^*_{\parallel} = 90^\circ \pm 1^\circ$ . This suggests that all of the films grew with approximately the same crystalline phase.

From the intensity and position of the diffraction peaks in the GIXD images of 20 nm samples, the full crystal structure can be obtained. Figure 2c shows a representative out-of-plane line scan (11L rod of a thiotetracene film grown at 60 °C on OTS-treated Si). This was obtained by slicing along the (11L) rod (at  $Q_{xy} = 1.33 \text{ \AA}^{-1}$ ) in the 2D intensity map. Several out-of-plane diffraction peaks were deconvoluted from the resulting spectrum using standard peak fitting software (after removal of the background). A self-consistent set of indices for the out-of-plane and in-plane diffraction spots was found (see Supporting Information), yielding the 3D unit cell geometry for thiotetracene films summarized in Table 1.<sup>33</sup> The GIXD results obtained for pentacene in this work (as shown in Table 1) are consistent with previously reported data.<sup>21,34,35</sup> Interestingly, thiotetracene exhibits the same in-plane unit cell as pentacene, while the lengths and alignment of the  $c$  axes are slightly different.

From the overall geometry of the thiotetracene unit cell and by assuming a close packed molecular layer, it can be concluded that there are two thiotetracene molecules per unit cell in a close to edge-on orientation. Even before any diffraction intensity analysis is performed, useful information on the alignment of these two molecules in the unit cell can be obtained. Most notably, the (10L) and (01L) peaks are missing in the GIXD

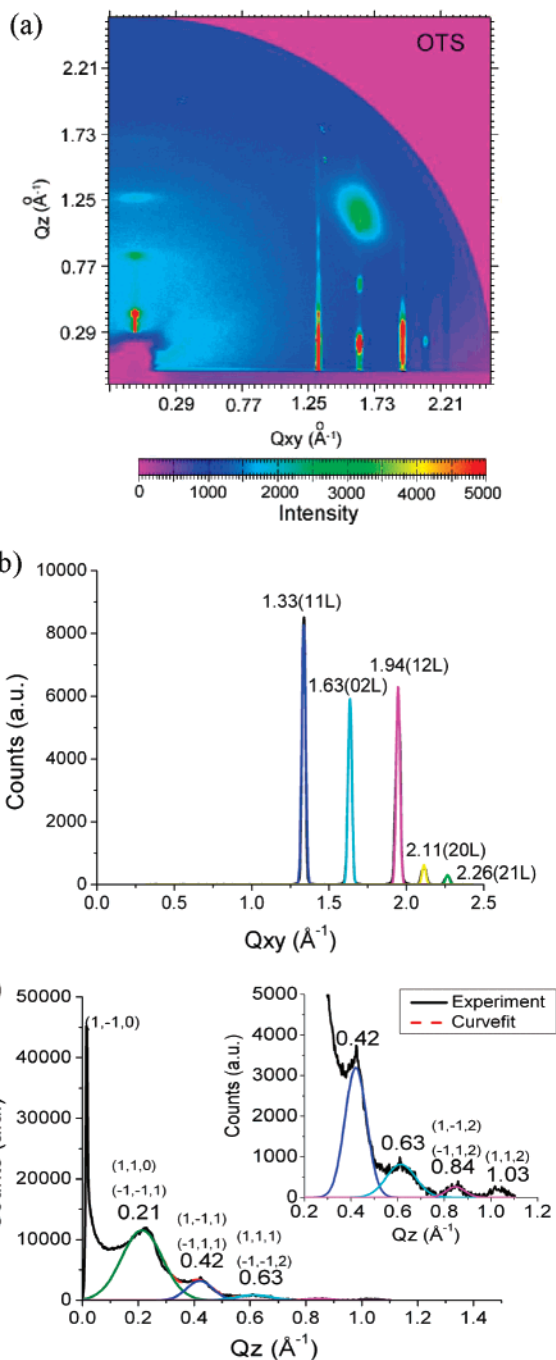


**Figure 2.** (a) 2D GIXD pattern of a 20 nm film of thiotetracene deposited at  $T_D = 60^\circ\text{C}$  on an OTS-treated Si substrate. The large green spot is due to diffuse scattering from the Si substrate. (b) The corresponding in-plane line scan of the GIXD signal integrated from  $Q_z = 0.0$ – $0.3 \text{ \AA}^{-1}$ . (c) The corresponding (11L) line scan of the GIXD signal. The experimental data and the deconvoluted spectrum of peaks are shown in the main graph. The inset is rescaled to show peaks in the high  $Q_z$  region. There is a strong diffraction peak near  $Q_z = 0 \text{ \AA}^{-1}$ . Because this peak's shape is affected by the total reflection, the exact  $Q_z$  value is unclear and thus not marked in the graph.

images in Figure 2 (i.e., missing in both the 2 nm as well as the 20 nm samples), which is indicative of a  $p2gg$  symmetry in the  $a$ – $b$  plane with a herringbone arrangement of two thiotetracene molecules. Such a herringbone arrangement of two molecules in the unit cell has also been observed in thin films of other oligoacenes such as pentacene.<sup>36</sup> It has to be noted though that strictly taken it is impossible to arrange two

(32) Hofmann, D.; Lengauer, T. *J. Mol. Struct.* **1999**, *474*, 13–23.

(33) Merlo, J. A.; Newman, C. R.; Gerlach, C. P.; Kelley, T. W.; Muires, D. V.; Fritz, S. E.; Toney, M. F.; Frisbie, C. D. *J. Am. Chem. Soc.* **2005**, *127*, 3997–4009.

(34) Fritz, S. E. Ph.D. thesis, The University of Minnesota, 2006.

(35) Yoshida, H.; Inaba, K.; Sato, N. *Appl. Phys. Lett.* **2007**, *90*, 1819301–1819302.

**Table 1.** Experimental Lattice Parameters Measured for Thiotetracene and Pentacene Thin Films<sup>a</sup>

compound	<i>a</i> (Å)	<i>b</i> (Å)	<i>c</i> (Å)	$\alpha$ (deg)	$\beta$ (deg)	$\gamma$ (deg)
tetraceno[2,3- <i>b</i> ]thiophene (thin film)	5.96	7.71	15.16	97.3	95.6	90
tetraceno[2,3- <i>b</i> ]thiophene (bulk) <sup>20</sup>	5.92	7.64	29.52	90	90	90
pentacene (thin film)	5.95	7.60	15.40	98.2	93.2	90
pentacene (thin film) <sup>21,34</sup>	5.91	7.56	15.54	98.4	92.8	90
pentacene (thin film) <sup>35</sup>	5.93	7.56	15.65	98.6	93.3	89.8
pentacene (thin film) <sup>27</sup>	5.96	7.60	15.61	98.8	93.4	89.8

<sup>a</sup> Literature values for bulk thiotetracene and pentacene films are also listed.

thiotetracene molecules in the unit cell such that two glide symmetry planes exist, due to the lack of symmetry in the thiotetracene molecule (due to the single thiophene unit). Apparently, the asymmetry introduced by the thiophene group does not contribute strongly to the overall in-plane scattering amplitude so that the in-plane symmetry detected by the X-ray diffraction is effectively  $p2gg$ . The missing of (01L) and (10L) peaks also indicates that the antiparallel configuration of the two molecules sitting in the same unit cell is less likely than the parallel configuration. This is in contrast to the orthorhombic structure reported for bulk thiotetracene crystals, where these two molecules have an antiparallel configuration. The length of the *c*-axis is almost twice the molecular length, and there are four molecules in one unit cell.<sup>20</sup> The differences between bulk and film structures could be due to the effect of the substrate on the thin film formation. Also note that the first peak in the (02L) scan (see Supporting Information) has a  $Q_z \neq 0$ , indicating a crystal structure quite different from the bulk crystal structure.<sup>20</sup> The orthogonality of the in-plane unit cell ( $\gamma = 90^\circ$ ) can be concluded from the degeneracy of the (11L) and ( $\bar{1}1L$ ) peaks. A high-resolution ( $0.01 \text{ \AA}^{-1}$ ) scan using a point detector (SSRL, BL 11-3) was performed on a sample from the same batch and did not reveal any splitting of the (11L) and (12L) peaks.

Using homemade software that implements a Simulated Annealing Monte Carlo minimization scheme, the energetically most favorable alignment of two thiotetracene molecules in a unit cell with the fixed, GIXD-determined unit cell geometry was calculated. The theoretically predicted optimal arrangement shows a herringbone-like alignment of the two molecules (Figure 3), in agreement with the experimentally observed extinction of the (01L) and (10L) diffraction peaks. The first molecule exhibits a tilt angle of  $4.1^\circ$  with respect to the surface normal; the second molecule exhibits a slightly larger tilt angle of  $9.6^\circ$ , resulting in an average tilt angle of  $6.9^\circ$ . The herringbone angle (angle enclosed by the planes of the two translationally inequivalent molecules) is  $49^\circ$ .

Using the diffraction intensities measured from the 20 nm thick films (values listed in Supporting Information), the molecular alignment in the unit cell was also calculated by crystallographic refinement (the residual,<sup>37</sup> differences between calculated and experimentally obtained diffraction intensities, was minimized). For that purpose, the calculated intensities were

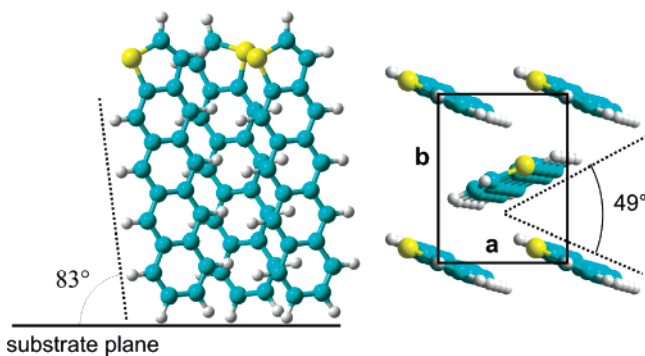


**Figure 3.** Thin film structure as predicted by the packing calculations, representing the lowest energy configuration of two thiotetracene molecules in a unit cell (fixed with experimentally obtained geometry from GIXD). In accordance with the missing (01L) and (10L) diffraction peaks, the two molecules are in a herringbone-like arrangement. Furthermore, the molecules are found to exhibit an average tilt of  $6.9^\circ$  with respect to the substrate surface normal and a herringbone angle of  $49^\circ$ .

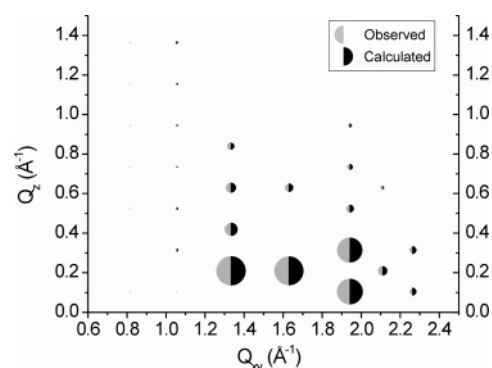


**Figure 4.** The measured and calculated diffraction intensity (best-fit crystallographic refinement) for the 20 nm thiotetracene film grown on an OTS-treated Si substrate. The intensity is indicated by the area of half-circles. An excellent fit is achieved by using the intensities measured from 28 experimental peaks and 9 fit parameters (3 angles for each molecule and the position of the second molecule with respect to the first molecule). The resulting average tilt angle of  $7.1^\circ$  for the molecules with respect to the surface normal is almost identical to that from the packing calculations ( $6.9^\circ$ ); the herringbone angle is about  $59.5^\circ$  ( $49^\circ$  from packing calculations).

corrected by application of appropriate Lorentz, polarization,<sup>38,39</sup> and Debye–Waller factors (the latter estimated from available pentacene data<sup>40</sup>). The resulting empirically determined alignment of thiotetracene molecules in the unit cell was nearly identical to that obtained from the packing calculations: the molecular tilt angles are  $3.7^\circ$  and  $10.5^\circ$ , and the herringbone angle is  $59.5^\circ$ . The simulated diffraction intensity and the experimental data are shown in Figure 4, illustrating the excellent agreement. The differences between the molecular packing from the crystallographic refinement and the packing calculations are quite small (tilt angles within  $1^\circ$  and herringbone within  $10^\circ$ ) and are likely within the experimental uncertainty of these methods.

Turning now to the 2 nm thin film samples, the Bragg rod profiles contain information on the molecular alignment in the film. By comparing the theoretical rod profiles (scaled structure factor squared) to the experimentally obtained one, we verify

(36) Drummy, L. F.; Miska, P. K.; Alberts, D.; Lee, N.; Martin, D. C. *J. Phys. Chem. B* **2006**, *110*, 6066–6071.

(37) Brunger, A. T. *Acta Crystallogr.* **1989**, *A45*, 42–50.

(38) Schlepütz, C. M.; Herger, R.; Willmott, P. R.; Patterson, B. D.; Bunk, O.; Bronnimann, C.; Henrich, B.; Hulsén, G.; Eikenberry, E. F. *Acta Crystallogr.* **2005**, *A61*, 418–425.

(39) Leveiller, F.; Jaquemah, D.; Leiserowitz, L.; Kjaer, K.; Als-Nielsen, J. *J. Phys. Chem.* **1992**, *96*, 10380–10389.

(40) Campbell, R. B.; Robertson, J. M.; Trotter, J. *Acta Crystallogr.* **1961**, *14*, 705–711.

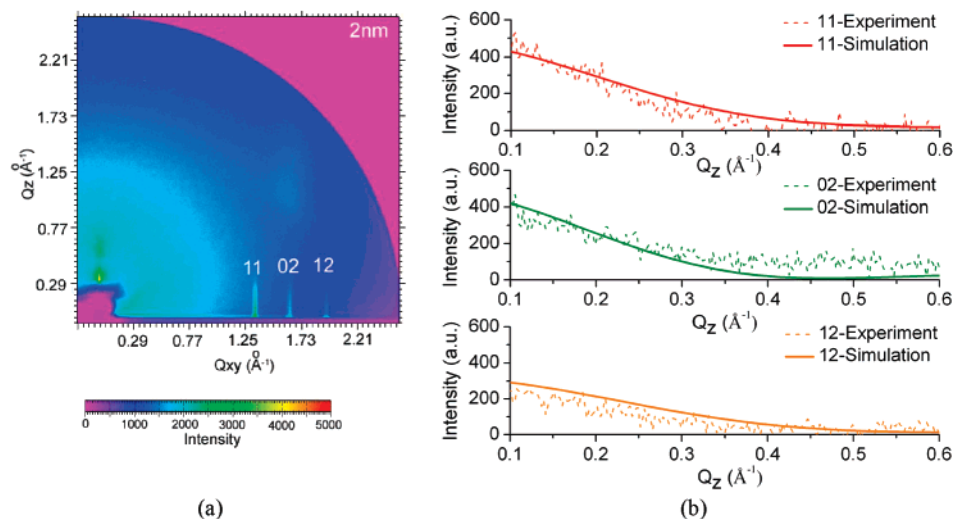


**Figure 5.** (a) 2D GIXD pattern of a 2 nm thiotetracene film, grown at 60 °C, on an OTS-treated Si surface. (b) Line scans along the (11), (02), and (12) rods from the GIXD image shown to the left. The intensity profile along these Bragg rods, which was calculated on the basis of the unit cell configuration obtained from the packing calculations, shows a good agreement. In this comparison, we have ignored the contribution of the second layer (about 20% coverage) in the 2 nm film, because this is small.

that the tilt angle in the 2 nm films is not significantly different from the tilt angle calculated for 20 nm thick films. A GIXD pattern of a 2 nm thick thiotetracene film grown at the substrate temperature of 60 °C on an OTS-treated Si substrate is shown in Figure 5a. Experimental and theoretical (11), (02), and (12) Bragg rod profiles, where the latter were calculated using the unit cell and molecular orientations obtained from 3D packing calculations, are shown in Figure 5b. The good match between the experimental data and the simulated Bragg rod profile suggests that the thiotetracene molecules in the 2 nm thin film exhibit a molecular tilt angle close to 7° (results from the packing calculations). This shows that the 2 and 20 nm thick thiotetracene films possess the same crystal structure, as suggested by the fact that the in-plane peak positions in the 2 and 20 nm samples are identical.

Using NEXAFS spectroscopy, we obtained an independent experimental verification of the tilt angle of the thiotetracene molecules. For linearly polarized X-rays, one can extract from the X-ray incidence angle dependence of the NEXAFS spectra the projections of the molecular distribution function.<sup>41</sup> For systems with crystalline order, like the thiotetracene films, it is therefore possible to determine experimentally the molecular tilt angle. We applied this technique to thin thiotetracene films originating from the same batch as the samples studied in the GIXD experiments. NEXAFS spectra were recorded using TEY mode,<sup>29</sup> normalized and corrected for finite polarization degree of the incident X-rays as discussed in the literature.<sup>41</sup>

The NEXAFS spectra of the 2 nm thin thiotetracene film grown at 60 °C on an OTS-treated silicon substrate are shown in Figure 6, exhibiting a clear incidence angle dependence. The resonances in the energy range between 284 and 286 eV are related to excitation of carbon 1s electrons to the unoccupied  $\pi^*$  orbital of the  $sp^2$ -hybridized carbon atoms in the benzene and thiophene rings, which are oriented perpendicular to the ring plane. The higher intensity of these  $\pi^*$  resonances for

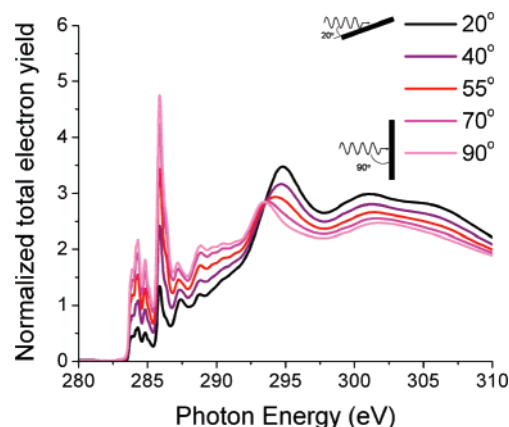


**Figure 6.** Normalized NEXAFS spectra for thiotetracene deposited at  $T_D = 60$  °C on an OTS-treated Si surface with a nominal thickness of 2 nm. The resonances between 284 and 286 eV correspond to the transition of  $\pi^*$  unoccupied C=C orbitals of bonds of the aromatic  $sp^2$ -hybridized carbon atoms in the benzene and thiophene rings<sup>41,42</sup> (four resonance peaks: 284.0 eV (partly from thiophene), 284.3 eV (benzene), 284.8 eV (thiophene), and 285.8 eV (benzene)).

normal incidence (90°) indicates that the molecules are oriented toward parallel to the surface normal. A quantitative analysis of the polarization dependence<sup>41</sup> yields a dichroic ratio of 0.69. This corresponds to an average tilt angle of 10° to the surface normal for the 2 nm thiotetracene film, thus supporting our GIXD-based structural model. The slightly larger tilt angle of the NEXAFS data could be indicative of the presence of noncrystalline areas in the film, which contribute to the NEXAFS measurements, but are invisible to GIXD.

The dichroic ratio in the NEXAFS spectra of the 20 nm thick films is slightly lower ( $\sim 0.6$ ), corresponding to an average molecular tilt angle of 15°. This indicates either a change of the molecular tilt angle with growing film thickness or, more likely, some roughening that occurs in the thicker films and which introduces a certain degree of 3D polycrystallinity, that is, grains whose  $a$ - $b$  plane is no longer exactly parallel to the substrate surface. The first explanation appears less likely, because the GIXD data and analysis show that the molecular packing and the tilt angles are nearly the same in the 2 and 20

(41) Stohr, J.; Samant, M. G. *J. Electron Spectrosc. Relat. Phenom.* **1999**, 98–99, 189–207.

(42) Stohr, J.; Gland, J. L.; Kollin, E. B.; Koestner, R. J.; Johnson, A. L.; Muetterties, E. L.; Sette, F. *Phys. Rev. Lett.* **1984**, 53, 2161–2164.

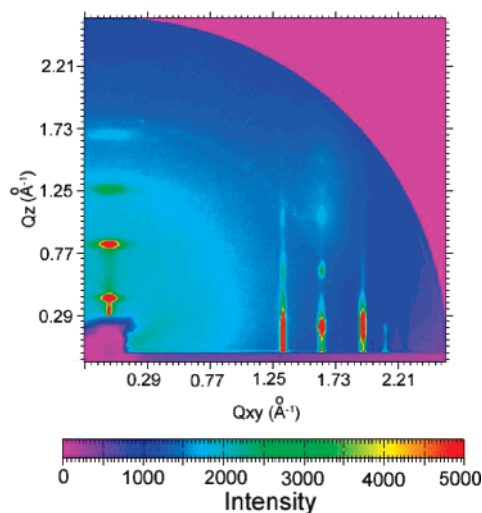


**Figure 7.** GIXD pattern for a thiotetracene thin film deposited at  $T_D = 60\text{ }^\circ\text{C}$  with nominal thickness of 20 nm on a plain Si substrate covered by a layer of native oxide. The thiotetracene lattice structure is the same as that of the film grown on an OTS-treated Si substrate (Figure 2). However, the film grown on the OTS-treated surface yields a diffraction pattern with higher signal-to-background ratio as compared to the one deposited on a plain Si substrate. This, together with the sharper diffraction peaks, indicates a higher degree of ordering for the OTS-treated surface.

nm films. Instead, the GIXD image of the 20 nm film (Figure 2b) shows some angular broadening of the (00L) peaks, both observations lending credit to the latter of the two possible explanations for the lower dichroic ratio in the thicker films.

Finally, the effect of substrate surface treatment prior to thiotetracene deposition on the crystallinity (i.e., the degree of spatial coherence of the thin film lattice) and transistor performance of 20 nm films is discussed. It has previously been observed that thin film transistor mobility greatly depends on surface chemical treatment for otherwise identical substrates.<sup>19,43</sup> Therefore, samples with thiotetracene films grown on Si substrate surfaces with and without OTS were investigated. Figure 7 shows a GIXD pattern obtained for a 20 nm thiotetracene film on a plain Si surface.

While the in-plane positions of the diffraction peaks are within the accuracy of the measurement, independent of the chemical substrate surface treatments, there appear to be different degrees of crystallinity in the respective thin thiotetracene films. This has been previously observed in thin films of various oligomeric semiconductor molecules.<sup>19</sup> As can be seen in Figures 2 and 7, the diffraction peaks of samples deposited on OTS surface at an elevated temperature ( $60\text{ }^\circ\text{C}$ ) exhibit a higher signal-to-background ratio as compared to that of films deposited at room temperature on untreated surfaces. Table 2 lists the measured thin film transistor (OTFT) performance (hole mobility) and full width at half-maximum (fwhm) of the GIXD (020) diffraction peak. The hole mobility of OTFT devices prepared from the same thin film deposition batch as the GIXD samples was extracted from current–voltage characteristics in the saturation regime by application of standard OTFT theory.<sup>44</sup> Because the (02L) peaks are well separated along  $Q_z$  and appear with sufficient intensity, the fwhm values were measured at the

**Table 2.**  $Q_{xy}$  fwhm's of the (020) Peak and Field-Effect Mobilities for Samples Deposited on Substrates with Different Surface Treatment<sup>a</sup>

	fwhm ( $\text{\AA}^{-1}$ )	mobility $L = 150\ \mu\text{m}$ ( $\text{cm}^2/\text{V}\cdot\text{s}$ )	mobility $L = 100\ \mu\text{m}$ ( $\text{cm}^2/\text{V}\cdot\text{s}$ )	mobility $L = 50\ \mu\text{m}$ ( $\text{cm}^2/\text{V}\cdot\text{s}$ )
plain, $25\text{ }^\circ\text{C}$	0.10	0.05	0.05	0.05
plain, $60\text{ }^\circ\text{C}$	0.08	0.06	0.04	0.06
OTS, $25\text{ }^\circ\text{C}$	0.09	0.08	0.10	0.10
OTS, $60\text{ }^\circ\text{C}$	0.06	0.21	0.31	0.31

<sup>a</sup> The fwhm was determined by peak-fitting to a Gaussian peak shape after background removal. The field-effect mobilities were extracted from the saturation regime of thin film transistor devices with different channel lengths ( $L$ ). The sample deposited on the substrate with OTS treatment at  $T_D = 60\text{ }^\circ\text{C}$  exhibits the smallest fwhm, and the corresponding OTFT device showed the best performance.

(020) peak. The fwhm is smaller for samples deposited at an elevated temperature on OTS-treated substrates, as compared to those deposited on plain substrates. From the inverse relationship between fwhm and crystalline coherence length, it follows that the thiotetracene films deposited under these conditions exhibit a higher degree of crystallinity. The observed correlation between crystalline quality of the film and favorable charge transport properties stresses the importance of high-quality films with large crystallites for high-performance thin film transistor devices.

## Conclusions

In summary, we investigated the thin film structure of vacuum-deposited thiotetracene thin films, which have been used for high performance organic thin film transistors. We have obtained detailed information on the molecular packing of the thiotetracene molecules in the thin film unit cell by application of a combination of theoretical and experimental techniques: GIXD and structure refinement of the diffraction data, energy minimization packing calculations, and NEXAFS. The results of these different methods are consistent and show that two thiotetracene molecules are oriented edge-on to the substrate surface, forming a herringbone packing motif. The average tilt angle was determined to be  $7^\circ$  relative to the surface normal, and the herringbone angle is about  $49\text{--}59^\circ$ . We found that a single phase (a triclinic unit cell with  $a = 5.96\ \text{\AA}$ ,  $b = 7.71\ \text{\AA}$ ,  $c = 15.16\ \text{\AA}$ ,  $\alpha = 97.30^\circ$ ,  $\beta = 95.63^\circ$ ,  $\gamma = 90^\circ$ ) exists in all samples with less than 20 nm thickness, and there is no phase change for samples grown at different substrate temperatures and with different surface treatment conditions. As compared to pentacene, the thiotetracene unit cell has the same in-plane geometry but a slightly different out-of-plane unit cell vector. The thin film crystallinity of thiotetracene significantly depends on fabrication conditions. High-temperature growth on OTS surface gives the best crystallinity as well as the best transistor mobility. The thin film structure of thiotetracene is different from that reported for bulk crystal structure.<sup>20</sup> This result indicates the importance of obtaining the thin film structure for understanding of structure property relationships for organic semiconductor thin film devices.

**Acknowledgment.** Q.Y. would like to thank Dean M. DeLongchamp from the National Institute of Standards and Technology for helpful discussions on NEXAFS. S.C.B.M. acknowledges postdoc fellowship support by the Deutsche Forschungsgemeinschaft (DFG) grant MA 3342/1-1. Z.B.

(43) Kline, R. J.; McGehee, M. D.; Toney, M. F. *Nat. Mater.* **2006**, *5*, 222–228.

(44) Horowitz, G.; Hajlaoui, R.; Bourguiga, R.; Hajlaoui, M. *Synth. Met.* **1999**, *101*, 401–404.

acknowledges partial financial support from the NSF-MRSEC (Center for Polymer and Macromolecular Assemblies), Air Force Office of Scientific Research (FA9550-06-1-0126), Sloan Research Fellowship, and Finmeccanica Faculty Scholar Fund. Part of this work was done at Stanford Synchrotron Radiation Laboratory (SSRL), a national user facility operated by Stanford University on behalf of the U.S. Department of Energy.

**Supporting Information Available:** Out-of-plane scans for thiotetracene; indices for in-plane and out-of-plane diffraction peaks; GIXD resolution; the measured intensity for diffraction peaks; and complete ref 6. This material is available free of charge via the Internet at <http://pubs.acs.org>.

JA0773002